DETECTION OF SPACE DEBRIS BY MEANS OF ATMOSPHERIC RADAR

Adila Wamisho

July 25, 2006

DETECTION OF SPACE DEBRIS BY MEANS OF ATMOSPHERIC RADAR

A thesis submitted to School of Graduate Studies Addis Ababa University in partial fulfilment of the requirement the Degree of Master of Science in Physics.

Adila Wamisho
Department of Physics
Faculty of Science
Addis Ababa University
June, 2006, Addis Ababa

Acknowledgment

I would like to acknowledge the following for their help through out the preparation of this thesis. First I thank God, Jehovah-jireh, who provides me what is possible and what is impossible in human eyes. My special thank must go to my advisor, Dr. Baylie Damtie, for he accepted me as his student at the beginning. I am grateful for his patience when I fail to understand and helped very mach when I look for his assistance in simulation. I am also thankful for he allowed me to work on his own personal computer with out which this paper had been very difficult.

A very special word of thanks is offered to Dr. Mulugeta Bekele, the former head of physics department at Addis Ababa University, who arranged conditions for me to work with my advisor at Bahir-Dar University. And to Dr. Tilahune Tesfaye, the present head of physics department at Addis Ababa University, for his help in the meantime.

I finally would like to thank my family, the Wamishos, for the day-to-day encouragement, prayer and wish. I appreciated the encouragement for my friends and form Elders and members of my Church, Mekanisa Addis Kidan Baptist Church.

Abstract

Space debris, which are resulted from space activities among other things, are potential-problems for the on going space science and development of space technology. A few alternatives in measuring, detecting, tracking and imaging space debris are there. Atmospheric signals contain signals scattered from space debris on top of signals scattered from the atmosphere. This thesis investigates how one can use atmospheric radar to detect space debris. The investigation is carried out by modelling the transmitted signal, the scattered signal for space debris in the presence of noise and also the impulse response of the receiver. We assume that the noise is white noise and for optimal detection we have employed matched filter at the receiver out put. The result shows that space debris can be easily detection by means of atmospheric radar.

Adila Wamisho: June, 2006, Addis Ababa

Preface

Man-made fragmentation are the potential problems of the on going development of space science and technology. To minimize hazards for the good of space science development detection and monitoring of space debris is very important. Investigations are going to meet the solutions for this problem. Many researches start with identification of space debris.

In this thesis we present how one can use atmospheric radar to detect space debris. The thesis is organized as follows: Chapter one gives some general introduction about radar and its fundamentals. In chapter two we give the background of space debris and go on to discuss the theoretical analysis of modelling space debris using radar. In chapter three we discuss how a signal from atmospheric radar may be used to detect space debris, which is essentially the aim of the thesis. Chapter four and five are dedicated for conclusion and future directions respectively.

Contents

Chapter 1

General Introduction

1.1 Overview of electromagnetic waves

Human beings have discovered many things from the mystery of nature. Investigations about nature are carried out in different fields of science. Physics, as a part of basic science, has played and is playing a very important role for the investigations. Several individuals have develop principles, theories and perform experiments which are very crucial for the findings and advancement of technology so far.

One of the remarkable physicists in the field of electromagnetism is James Clerk Maxwell (1831-1879), a Scottish. In 1856 he wrote his famous theoretical paper on electromagnetic waves. In this scientific publication, he proposed the possible existence of electromagnetic waves and at the same time postulated that if such waves could ever be produced, they would travel through free space with the speed of light . According to Maxwell, light itself propagates as an electromagnetic wave. The electromagnetic waves, he was expecting to be produced, should differ from light only in their frequency but not in their speed. Maxwell gave no clues as to how such waves might be generated or detected. Even his famous equations has nothing to do with the generation and detection of these waves, only the propagation. As a result, his significant paper remain a blue-print until the time of Heinrich Rudolf Hertz (1857-1894), a German. In 1888 Hertz confirmed Maxwell's theory in his series experiments in which he not only produced and detected electromagnetic waves but also demonstrated their properties as any wave. Hertz experiment led to the development of many electronic devices such as radio, TV, radar and so on. This thesis investigates how one can use atmospheric radar to detect space debris in near Earth environment.

1.2 Overview of radar

The word radar is an acronym for RAdio Detection And Ranging. And may be defined as the art or technique of determining objects (targets) by means of radio waves reflection. Since, at the beginning radar was meant for detecting and ranging objects. The idea of radar has been around for a long time before it was actually developed [1 and 2]. In 1900 Nikola Tesla wrote about the use of reflection of electric wave, like sound echo, to determine the relative position or course of a moving object such as a vessel at sea . In 1904, Christian Hulsmeyer, a German, proposed the use of radio echoes in detecting devices designed to avoid collision in marine navigation. In 1924 Sir Edward Vector Appleton, a British, has done successful radio range finding experiment when he used radio echoes to determine the height of the ionosphere (i.e an ionized layer of the upper atmosphere which can reflect radio waves).

Perhaps radar was one of the most important electronic devices developed during World War II. One may say a practical radar system was made by Sir Robert Watson-Watt, a British, in 1935. And England established radar stations during the war. In addition to England, the development of radar system has been carried out independently in Germany, United States, Russia, France, Italy, and Japan in the time of the war. Radar has now many applications: Defense, meteorology, early warning system, mapping, air-traffic control, ship and aircraft navigation, altimeter on aircraft, traffic police speeding control, mineral and land-mine exploration, space debris measurement, which we mainly consider in this thesis, and so on.

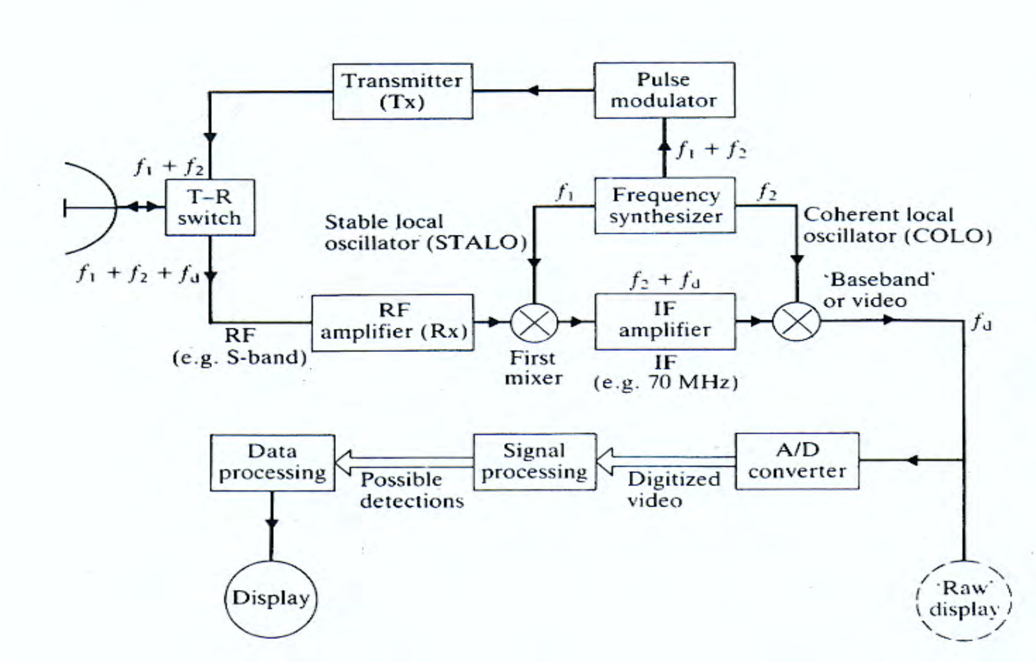

Figure 1.1: Block diagram of pulsed radar system

1.3 Basic components of radar

Radar system consists of transmitter and receiver. Transmitter transmits a modulated waveform through the directive antenna into a specific volume to search for target. A portion of the transmitted signal with its all modification and the noise is reflected back. Receiver receives the returned signal through the antenna and processes it [3, 4, and 5]. A pulsed radar system is shown in figure 1.1

One may list the basic components of a radar system as antenna, duplexer, oscillator, mixers, filter, amplifier, waveform generator, and signal processor. Antenna is used to transmit and receive signals. The antenna is focussed to a specific direction in order to use the radar power effectively. Duplexer switches the antenna between transmission and reception. In the case of pulsed monostatic radar, one can not receive and transmit simultaneously. When transmitter is on for a short period of time, which is determined by the pulse width, the duplexer switches off the receiver. During reception the duplexer switches off the transmitter. The oscillator provides the carrier wave for the radar.

This wave is usually with high frequency. The mixers modulate carrier signal in accordance with the radar waveform in the transmitter and remove the high frequency signal in the receiver by mixing it with the carrier and then passing it into the low pass filter. Filter is used to filter out unwanted signals like noise. Amplifiers increase the power in the signal. Waveform generator produces the desired waveform for modulation. The waveform is also used as a matched filter using its replica. Signal processor detects, identifies, estimates the range and/or Doppler shift of the targets, removes clutter and noise not removed earlier by the filter. Since analog to digital (A/D) converters are more accurate, signal processing is usually done digitally. Sampling should be done in accordance with the Nyquist theorem.

1.4 Radar frequencies

Radar uses radio waves of different frequencies depending on the mission and the functionality of the radar. Radar operating frequency is usually used in classification of radars [6]. These classifications are shown in Table 1.1

1.5 Radar equation

The radar equation is useful for both understanding of the radar operation and designing a specific radar system [6, 7, and 8]. To find out radar equation for a point target, consider a radar with omnidirectional antenna, i.e radiating energy equally in all direction, spherical radar pattern. The peak power density (P_D) at any point or distance (R) is given by

$$P_D = \frac{P_t}{4\pi R^2}, \tag{1.1}$$

where P_t is the peak transmitted power and $4\pi R^2$ is the surface area of a sphere of radius R. Usually radar system implement directional antennas in order to focus the power density into specific region. This focusing power of the antenna is measured by the gain (G) of the antenna, which is given by

$$G = \frac{4\pi A_e}{\lambda^2}, \tag{1.2}$$

Table 1.1: Radar frequency bands.

Letter designation	Frequency (GHz)
HF	**0.003 - 0.03**
VHF	**0.03 - 0.3**
UHF	**0.3 -1.0**
L-band	**1.0 - 2.0**
S-band	**2.0 - 4.0**
C-band	**4.0 - 8.0**
X-band	**8.0 - 12.5**
Ku-band	**12.5 - 18.0**
K-band	**18.0 - 26.5**
Ka-band	**26.5 - 40.0**
MMW	**Normally > 34.0**

where λ is the wavelength of the transmitted wave and A_e is the antenna effective aperture. The power density at a distance R away from a radar using a directive antenna of G is then given by

$$P_D = \frac{P_t G}{4\pi R^2}. \tag{1.3}$$

The radar cross section, which is denoted by σ, refers to target specification parameter (i.e target size, orientation, physical shape, and material). It can be complex function of target specifications parameters. Since, it depends on the angle one views the target. For instance, a rectangle viewed from the side is a line, a box viewed from one of its face is a rectangle, a sphere viewed from any side is the same. The radar cross section is given by

$$\sigma = \frac{P_r}{P_D}, \tag{1.4}$$

where the unit of σ is in m^2 and P_r is the power reflected from the target. The total power received by the radar $P_{Dr}$is then given by

$$P_{Dr} = \frac{P_t G \sigma}{(4\pi R^2)^2} A_e. \tag{1.5}$$

Substituting the value of A_e from equation (1.2) into equation (1.4), one obtains

$$P_{Dr} = \frac{P_t G^2 \lambda^2 \sigma}{(4\pi)^3 R^4}. \tag{1.6}$$

Equation (1.6) is usually called the radar equation for a point target. We can find out the maximum radar range R_{max}, the distance above which the target can not be detected. If the minimum detectable signal power is S_{min}, then one can easily obtain

$$R_{max} = \left(\frac{P_t G^2 \lambda^2 \sigma}{(4\pi)^3 S_{min}} \right)^{1/4}. \tag{1.7}$$

In practical situation the returned signal received by the radar is corrupted by noise. Therefore the power of the noise must be considered in derivation of the radar equation. The signal-to-noise ration (SNR) at the output may be defined by

$$SNR = \frac{P_t G^2 \lambda^2 \sigma}{(4\pi)^3 k T_e B F L R^4}, \tag{1.8}$$

where $k = 1.38 \times 10^-23 J/k$ (*Boltzman constant*), T_e is effective noise temperature in degree kelvin, B is radar band width in Hertz, F is noise figure (noise of the receiver), and L is total radar losses. One can follow a similar procedure to derive the radar equation for extended target.

1.6 Radar ambiguity function

Radar ambiguity function is used by radar designers most to study the effectiveness of different radar waveforms which may suit for various radar application [6,7, and 8]. It is also used to determine the range and the speed (Doppler shift) resolution, which is one of the limitations of a radar, for a specific radar waveform. We know that incoherent scatter signal deformed (corrupted) by the impulse response of the receiver, and therefore, the impulse response affects the signal autocorrelation function. A second factor which deform the signal and its autocorrelation function is the radar modulation since it determine the scattering altitudes of elementary signal contributing to the total signal at a given instant of time [9]. The control mechanism for this is introducing the discussion of radar ambiguity function. The radar ambiguity function provides us the technique to increase the performance of the radar out of this limitation. Let $s(t)$ be the signal of a radar system. The energy of the signal is given by

$$E = \int_{-\infty}^{\infty} |s(t)|^2 dt. \tag{1.9}$$

And then, the two-dimensional (2-D) correlation function from the matched filter response is given by

$$\chi(\tau; f_d) = \int_{-\infty}^{\infty} s(t) s^*(t+\tau) e^{j2\pi f_d t} dt, \tag{1.10}$$

where τ is the time delay and f_d is the Doppler frequency shift due to the motion of the target. The radar ambiguity function for the signal $s(t)$ is defined as the modulus squared of the 2-D correlation function. That is given by

$$|\chi(\tau; f_d)|^2 = \left| \int_{-\infty}^{\infty} s(t) s^*(t+\tau) e^{j2\pi f_d t} dt \right|^2. \tag{1.11}$$

The radar ambiguity function has the following properties:

1. The maximum value for the ambiguity function occurs at $(\tau; f_d) = (0;0)$,

$$max\{|\chi(\tau; f_d)|^2\} = |\chi(0;0)|^2 = 4E^2. \tag{1.12}$$

$$|\chi(\tau; f_d)|^2 \leq |\chi(0;0)|^2. \tag{1.13}$$

   where E is the energy of the signal.

2. The ambiguity function is symmetric,

$$|\chi(\tau; f_d)|^2 = |\chi(-\tau; -f_d)|^2. \tag{1.14}$$

3. The total volume under the ambiguity function is constant,

$$\iint |\chi(\tau; f_d)|^2 d\tau df_d = 4E^2. \tag{1.15}$$

4. If the function S(f) is the Fourier transform of the signal $s(t)$, then by using Parseval's theorem

$$|\chi(\tau; f_d)|^2 = \left| \int S^*(f) S(f - f_d) e^{j2\pi f_d t} df \right|^2. \tag{1.16}$$

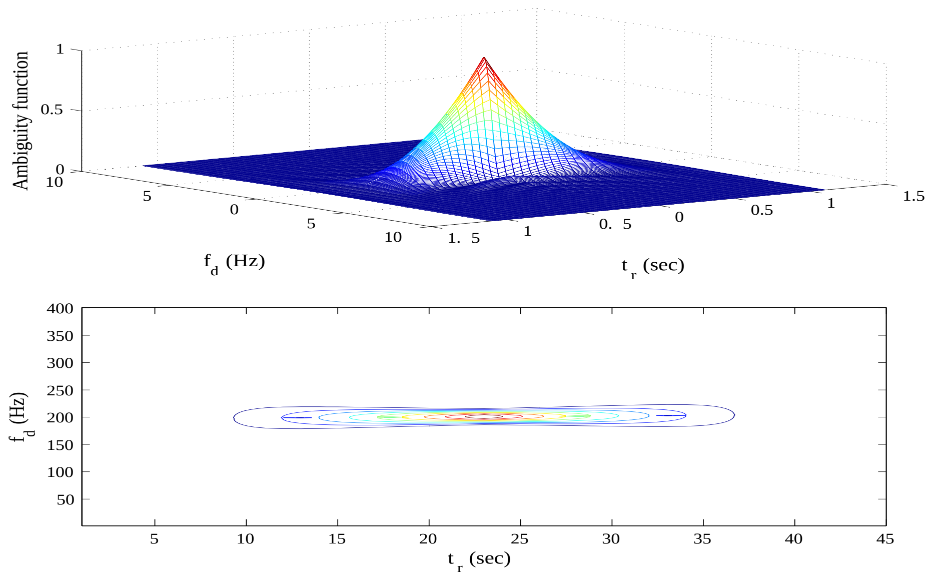

Figure 1.2: Ambiguity function plot: Top panel shows the ambiguity function in 3D. Bottom panel shows the corresponding contour plot.

The ideal radar ambiguity function is an infinitesimal width peak at the origin and zero elsewhere. This means that it provides perfect resolution, capability of determining targets as distinct objects what-so-ever they are close. Practically this is impossible. The practical radar ambiguity function has the form of Sinc function, $sin(x)/x$ [6].

Consider normalized rectangular pulse $s(t)$ defined by

$$s(t) = \frac{1}{\sqrt{\tau'}} Rect\left(\frac{t}{\tau'}\right), \tag{1.17}$$

where τ' is the pulse width. Using equation (1.10), the correlation function is,

$$\chi(\tau; f_d) = \int_{-\infty}^{\infty} s(t)s^*(t+\tau)e^{j2\pi f_d t}dt \tag{1.18}$$

Using equation (1.11), and performing the integration yield,

$$|\chi(\tau; f_d)|^2 = \left|\left(1 - \frac{|\tau|}{\tau'}\right) \frac{sin(\pi f_d(\tau' - |\tau|))}{\pi f_d(\tau' - |\tau|)}\right|^2 \text{ for } |\tau| \leq \tau' \tag{1.19}$$

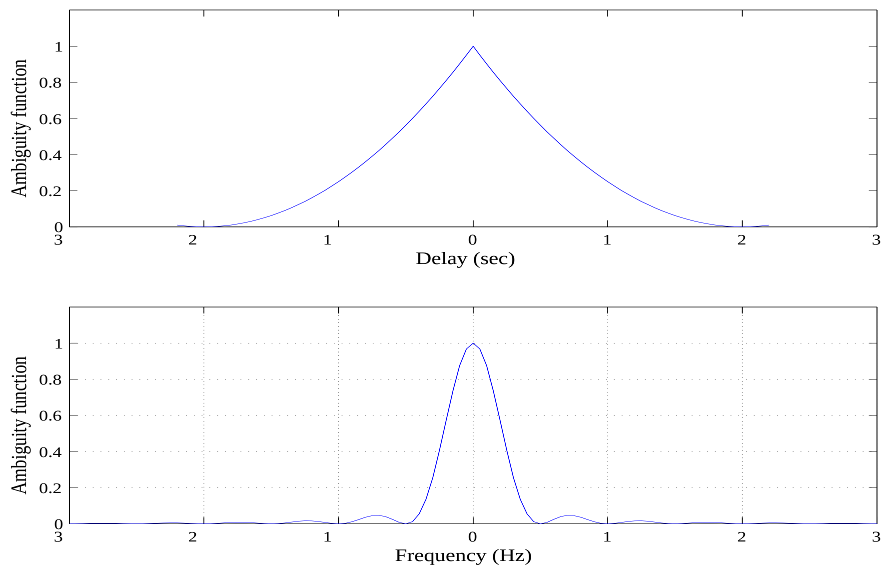

Figure 1.3: Ambiguity function plot. Top panel shows cut along the Doppler axis. Bottom panel shows cut along the delay axis.

The ambiguity function cut along the time delay axis τ can be obtained by setting $f_d = 0$. That is,

$$|\chi(\tau; f_d)|^2 = \left(1 - \frac{|\tau|}{\tau'}\right)^2 \text{ for } |\tau| \leq \tau^{'} \tag{1.20}$$

The ambiguity function cut along the Doppler axis f_d can be obtained by setting $\tau = 0$. That is,

$$|\chi(0; f_d)|^2 = \left|\frac{sin(\pi\tau^{'} f_d)}{\pi\tau^{'} f_d}\right|^2 \tag{1.21}$$

Figure 1.2 shows the ambiguity function in 3D and its corresponding contour plot defined by Eq.(1.19). Figure 1.3 shows that the plot of ambiguity function cuts defined by Eq.(1.20) and Eq.(1.21). From these figures one can see that the zero Doppler cut along the time delay axis extended between $-\tau^{'}$ and $\tau^{'}$, where we assume $\tau^{'} = 2sec$. This implies that close target would be ambiguous if they are separated by less than $\tau^{'}$.

Chapter 2

Space Debris

2.1 Introduction

Now the days the outer Earth environment is becoming a crowd of objects which are orbiting the Earth. These are operational (giving useful function) and none operational (giving no longer useful function). Objects which no longer serve any useful purpose referred to as space debris. There are many sources of space debris. The main source is space activity by human beings. The discarded hardware from launch vehicles upper stages have been left on orbit after they are spent. Many satellites are also abandoned at the end of useful life. Other sources are fragmentation as a result of explosions and collisions in space, firings of satellite solid-rocket motors, material ageing effects, and leaking thermal-control system [10, 11, and 12].

Since Sputnik's launches, 1957, there have been more than 4000 rocket launches. According to U.S Space Command and European Space Agency (ESA), approximately 200 000 objects larger than 1 cm currently orbiting the Earth, which are the remainders of the space activity over these years. The larger objects (i.e larger than 10 cm), trackable objects, have known orbits and currently monitor by the U.S Space Surveillance Network, but information about the small-sized debris is fragmentary and mainly statistical. These fragmentation can be assumed as schematics diagram shown figure 2.1.

Space debris are potentially dangerous and near-Earth space is already at risk from human space activity. And it is in a great need of protection from the responsible (sci-

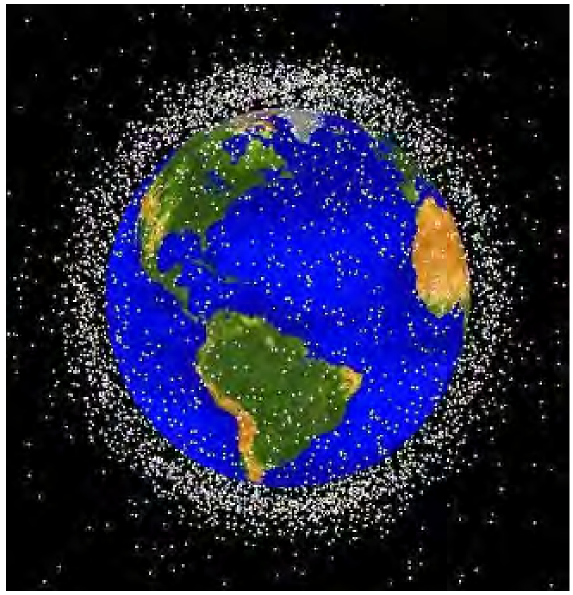

Figure 2.1: Schematics space debris catalog near Earth.

entists, governments, and intonational community). For the above mentioned reason it is vital to detect space debris. When one think of detection, measuring comes first.

2.2 Measuring space debris

Remote sensing of space debris from ground-based measurements may fall into optical measurement or radar measurement. Since debris in geostationary orbit (GEO) all move in the same direction (equatorial orbit) and at almost similar speed, collision at this altitude are less distractive. Objects in GEO are very far in distance from Earth and have mach more stable orbit than Low Earth Orbit (LEO). That is, the debris in GEO are potentially more permanent and longer hazardous life time. The debris situated in GEO appears to be at least to orders of magnitude less severe than that in LEO. Thus, current collision risk in GEO are lower than in LEO but due to the long life time of fragment on GEO in comparison to LEO the environmental consequences of a collision become great [11].

Results show that an optical telescope of modest size can outperform most radar for detection of debris at GEO. LEO is the most crowded region with operational satellite and debris, and is therefore a greater hazard. There are many possible orbit and higher relative velocity. LEO is also the area where extra-vehicular activities are most likely to take place and where the International Space Station located. Moreover, larger constellations of communication satellites are prepared for launch, due to the demand of communication the population of operational satellites are expected to grow. These space satellites may collide with space debris such as French Cerise reconnaissance satellites. Results in general show that radar outperform optical telescopes for space debris measurement in LEO.

Space debris can be detected by an optical telescope when the debris object is sunlit and the sky background is dark. For object in LEO, this time period is limited just after sunset or before sunrise, that is one or two hour. But for debris object in GEO the above limitation time become the entire night time. This is the fact that optical measurement outperform radar measurement for space debris in GEO. Optical telescopes which are implemented have a capability of detecting debris not smaller that 1m, but in GEO there are still debris smaller than 1m resulted from explosion.

Space debris can be detected by radar and this may be advantageous because of radar all-weather and day-and-night performance. It is due to this fact that radar measurement out perform optical one for objects in LEO. The radar power budget and operating wavelength are limiting factors for detection of small objects at long ranges.

Basically two types of radars are used for space debris measurement. These are mechanically and electrically controlled beam direction radars. Radar with mechanically controlled beam direction uses parabolic reflector antenna. Only objects in actual filed of view given by the mechanical direction of the parabolic reflector can be detected and measured. Radar with electrically controlled beam direction uses phased array antenna. Multiple objects at different can be detected and measured simultaneously [10 and 11].

2.3 Radar cross section of a space debris

The theoretical analysis of space debris using radar measurement may start from radar equation for point target, Eq.(1.6) in section (1.5). As we have discussed, a radar cross

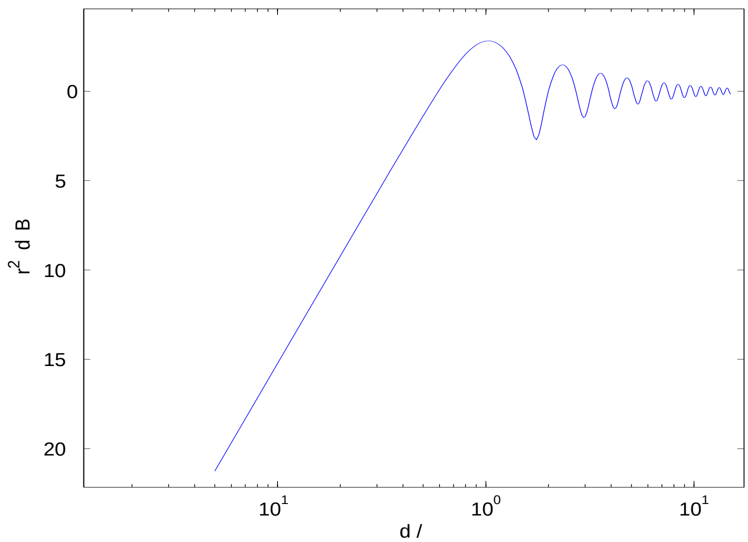

Figure 2.2: The relation between radar cross section and target dimension.

section (σ) can be a complex function of target specification such as shape [6 and 12]. For simplicity, we can assume a debris particle to be sphere of diameter d. For a Rayleigh region, the smaller diameter, the radar cross section is proportion to d^6. For optical region, larger diameter, the radar cross section is just the geometrical cross section, $\frac{1}{4}\pi d^2$. For Mie region, the mediator, the radar cross section shows an oscillatory behavior. It is known that the Rayleigh approximation is valid if the diameter is less than one fifth of the wavelength and the optical approximation is valid if the diameter is larger than ten times the wavelength of the transmitted wave (signal) [6] and [12] . Using these argument the radar cross section is given by

$$\sigma = \begin{cases} \frac{9\pi^5}{4\lambda^4} d^6, & \text{when } d < \lambda/(\pi\sqrt(3)), \\ \frac{1}{4}\pi d^2, & \text{when } d > \lambda/(\pi\sqrt(3)), \end{cases} \tag{2.1}$$

where λ is the wavelength of the transmitted wave. The relation between radar cross section and target diameter is shown in figure 2.2.

2.4 Modelling the radar measurement

We know that pulse radar use modulation envelop and carrier signal. This means that the transmitted signal of the radar can be represented by,

$$S_t(t) = env(t).exp(i\omega_r t), \tag{2.2}$$

where $env(t)$ is the transmission envelope, and ω_r is the radar radio frequency. If the debris particle is assumed to be a point target at a range R_o the received signal, $S_r(t)$ is just the delayed, by $2R_o/c$, and attenuated version of the transmitted signal. Where c is the speed of light, therefore the received signal is given by,

$$S_r(t) = A_o.S_t(t - 2R_o/c), \tag{2.3}$$

where A_o is a constant account for the modification of the signal such as attenuation. Eq.(2.3) represents the signal that just reached at the receiver antenna. Here at the receiver signal frequency is first translated to some translational frequency, ω_t, and the signal become S_{rt}. This is done by frequency mixing. Let us take the signal $exp(-i\omega_1 t)$ as mixing signal, then from Eq.(2.3), we get

$$S_{rt}(t) = S_r(t) * exp(-i\omega_1 t) = A_o.env(t - 2R_o/c).exp(i\omega_t).exp(-i\omega_r 2R_o/c), \tag{2.4}$$

where $\omega_t = \omega_r - \omega_1$. If $h(t)$ is impulse response of the matched filter of the received, the signal become the convolution of the two

$$s(t) = h(t) * S_{rt}(t - 2R_o/c) = A_o.h(t) * env(t - \frac{2R_o}{c}).exp(i\omega_t).exp(-i\omega_r \frac{2R_o}{c}), \tag{2.5}$$

where $*$ is convolution operation. We can assume that during the beam passage the target has constant radial acceleration, a_o. The target range is then given by, using equation of motion

$$R(t) = R_o + v_o t + \frac{1}{2}a_o t^2, \tag{2.6}$$

where R_o is initial range and v_o is the initial velocity at time $t = 0$. For a slowly moving target during the beam passage, we can replace $R(t)$ by R_o in Eq(2.5) and we have

$$s(t) = A_o.h * env(t - \frac{2}{c}(R_o + v_o t + \frac{1}{2}a_o t^2)).exp(i\omega_t t).exp(-i\omega_r \frac{2}{c}(R_o + v_o t + \frac{1}{2}a_o t^2)). \tag{2.7}$$

Here, Eq.(2.7) can be rewritten for simplicity as,

$$s(t) = A_o.h * env(t - \frac{2}{c}R(t)).exp(-i\omega_r \frac{2R_o}{c}).exp(-i\omega_o t).exp(-i\alpha_o t^2), \tag{2.8}$$

where

$$\omega_o = 2v_o\omega_r/c, \tag{2.9}$$

and

$$\alpha_o = a_o\omega_r/c. \tag{2.10}$$

Here we assume that the transmission $S_t(t)$ in Eq.(2.2) is directly available as a transmission sample signal to use it in the time of signal processing. The expression $exp(i\omega_t t)$ in Eq.(2.7) is dropped in Eq(2.8), since it is would be normalized to unity in computing the determining factor in Eq(2.26).

2.5 Modelling signal corrupted by noise

Our measurement will not be, by no means, clear of noise. Therefore modelling of the signal should consider this fact. Noise is random by its nature. It means that there is a random variable in our measurement, so do in our modelling [15 and 18]. The signal containing noise may be given by

$$m(t) = s(t) + n(t) \tag{2.11}$$

where $m(t)$ is the measured signal and $n(t)$ is the noise. It is common knowledge to assume Gaussian noise [6] and [18]. Since the noise is random the mean value is zero and it has some variance $\sigma^2/2$. The probability density $D(n)$ is given by

$$D(n) = \frac{1}{\pi\sigma^2}.exp(-\frac{1}{\sigma^2|n|^2}). \tag{2.12}$$

Using normalization it is possible to relate the variance and noise power P_n and it is given by

$$P_n = E|n|^2 = \sigma^2 \tag{2.13}$$

The autocorrelation of the noise is given by

$$\bar{n}_i(t) = \int_{-\infty}^{\infty} n_i^*(t)n_i(t+\tau')d\tau' = \frac{N_o}{2}\delta(t) \tag{2.14}$$

where N_o is some constant and $\tau^{'}$ is the delay. This means that the noise samples $n_k = n(k\tau)$ for the maximum sampling interval τ are not correlated. The sampling measurements $m_k = m(k\tau)$ are statistically independent. If we denote the joint conditional probability density of m_k, given s_k by $D(m_k|s_k)$ it would be then given by

$$D(m_k|s_k) = \frac{1}{\pi\sigma^2} exp(-\frac{1}{\sigma^2}|m_k - s_k|^2). \tag{2.15}$$

If there are K samples (measurements) taken the posterior probability distribution is the product of the individual using Bayesian statistics [13] and [14], given by

$$D(\mathbf{m}|\mathbf{s}) = \prod_{k=0}^{K-1} D(m_k|s_k) = \frac{1}{(\pi\sigma^2)^K} exp(-\frac{1}{\sigma^2} \parallel \mathbf{m} - \mathbf{s} \parallel^2) \tag{2.16}$$

2.6 Parameter estimations using inversion

Our parameters in the measurement (A, R, ω, and α) can not be resolved directly from the measurements rather we find the joint probability distribution of them. The randomness of the problem makes the solution to be difficult in many cases [15 and 17]. Mathematically, random problems can be handle by the Bayasian statistics for the modelling purpose. Bayesian approach in modelling a measurement have some futures which are very helpful in answering questions one may ask in analyzing the data. The model in Bayes' approach is random and the solution is probability distribution for the model parameters. This probabilistic distribution for the model parameters and it used to answer questions about the model parameters. This modelling allows one to incorporate prior information which may come from other things such as experience, even if this is not scientific [13, 14, and 18].

The inverse problem is to find the joint probability density of the signal of parameters A, R, ω, and α given a measurement $\mathbf{m}$. This is denoted by $D(\mathbf{m}|\mathbf{s})$ or $D_p(\mathbf{m}|\mathbf{s})$ is called the posterior density from Bayesian approach and is given by using Eq.(2.16)

$$D(\mathbf{m}|\mathbf{s}) = D(\mathbf{m}|A, R, \omega, \alpha) = \frac{1}{(\pi\sigma^2)^K}.exp(-\frac{1}{\sigma^2} \parallel \mathbf{m} - \mathbf{s} \parallel^2) \tag{2.17}$$

The exponential in Eq.(2.17) is the likelihood function $\mathcal{L}$, and it is given by

$$\mathcal{L} = \mathcal{L}(A, R, \omega, \alpha) = -\frac{1}{\sigma^2} \parallel \mathbf{m} - \mathbf{s}(A, R, \omega, \alpha) \parallel^2 \tag{2.18}$$

The joint probability density of the signal and the measurement $D_{sm}(\mathbf{s}, \mathbf{m})$ is the solution for our parameters. From the property of the conditional probability the joint density is given by

$$D_{sm}(\mathbf{s}, \mathbf{m}) = D(\mathbf{s}|\mathbf{m})D_s(\mathbf{m}) = D(\mathbf{m}|\mathbf{s})D_m(\mathbf{s}) \tag{2.19}$$

where

$$D_s(\mathbf{m}) = \int D_{sm}(\mathbf{s}, \mathbf{m})d\mathbf{s}, \tag{2.20}$$

and

$$D_m(\mathbf{s}) = \int D_{sm}(\mathbf{s}, \mathbf{m})d\mathbf{m}. \tag{2.21}$$

The solution for the Eq.(2.19) gives the Bayes inversion formula

$$D_p(\mathbf{s}|\mathbf{m}) = \frac{1}{D_s(\mathbf{m})}.D_m(\mathbf{s}).D(\mathbf{m}|\mathbf{s}), \tag{2.22}$$

where $D_m(\mathbf{s})$ is the prior density, which describes the relative frequency of the parameters in the target population. The joint density D_{sm} is what we like to find out to estimate the parameters statistically. D_{sm} can not be solved directly rather assuming some function D_{pr} of the form D_{sm} and test it if it matches with D_{sm}. For simplicity we can assume uniform prior distribution. By then we have fixed D_{pr} and $D(\mathbf{m}|\mathbf{s})$, the factor in Eq.(2.22) can, possibly, be determined with the condition, $D_p(\mathbf{s}|\mathbf{m})$ is a normalized probability density.

$$D(A, R, \sigma, \alpha|\mathbf{m}) = C(\mathbf{m})exp(L(A, R, \omega, \alpha, \mathbf{m})) = C(\mathbf{m})exp(-\frac{1}{\sigma^2} \parallel \mathbf{m} - (A, R, \omega, \alpha) \parallel^2), \tag{2.23}$$

where C is constant, normalization factor, which dose not depend on A, R, ω and α. The posterior density is the solution of the problem. That means, if the actual target parameters are A_o, R_o, ω_o, α_o, we expect that the posterior density would be well concentrated around the point (A_o, R_o, ω_o, and α_o). The parameters can be assumed as a vector ($\hat{A}$, $\hat{R}$, $\hat{\omega}$, $\hat{\alpha}$) that maximize the posterior density with $\mathbf{m}$ given. The maximum of the posterior density D_p results the determining tool for the parameters. This can be given by

$$\parallel D_p \parallel = \parallel C \parallel .exp(-\frac{1}{\sigma^2} \parallel \mathbf{m} - s(A, R, \omega, \alpha) \parallel^2). \tag{2.24}$$

Rearranging Eq(2.24) yields

$$-\sigma^2 exp(- \parallel \frac{D_p}{C} \parallel) = \parallel \mathbf{m} \parallel^2 + \left| \parallel \mathbf{s} \parallel^2 - \frac{< \mathbf{m}, \mathbf{s} >}{\parallel \mathbf{s} \parallel} \right|^2 - \left| \frac{< \mathbf{m}, \mathbf{s} >}{\parallel \mathbf{s} \parallel} \right|^2. \tag{2.25}$$

The last expression in Eq.(2.25) is a determining tool which does not depend on the signal amplitude A

$$\frac{|<\mathbf{m}|\mathbf{s}>|}{\parallel \mathbf{s} \parallel} = \frac{|<\mathbf{m}, A.exp(R,\omega,\alpha)>|}{\parallel A.exp(R,\omega,\alpha) \parallel} = \frac{|<\mathbf{m}, exp(R,\omega,\alpha)>|}{\parallel exp(R,\omega,\alpha) \parallel} \tag{2.26}$$

Two things must be done here, the first is to maximize the determining tool

$$(\hat{R},\hat{\omega},\hat{\alpha}) = max\left|\frac{<\mathbf{m}|\mathbf{s}>}{\parallel \mathbf{s} \parallel}\right| \tag{2.27}$$

and the second is to select the amplitude A in $\mathbf{s} = A.exp(R,\omega,\alpha)$ in such a way that the second term in Eq.(2.25) become zero, that is

$$\hat{A} = \frac{<\mathbf{m}, exp(\hat{R},\hat{\omega},\hat{\alpha})>}{\parallel exp(\hat{R},\hat{\omega},\hat{\alpha}) \parallel^2} \tag{2.28}$$

Form Eq.(2.8) the signal is given by

$$\parallel \hat{\mathbf{s}} \parallel = \parallel \hat{A}.exp(\hat{R},\hat{\omega},\hat{\alpha}) \parallel \tag{2.29}$$

The signal energy is the sum of square of the individual signal samples and it is given by

$$W_s = \sum \tau |s_n|^2 = \tau \parallel \mathbf{s} \parallel^2 . \tag{2.30}$$

The noise power is given in Eq.(2.13), section(2.5). And therefore the signal-to-noise ratio(SNR) is then given by

$$S\hat{N}R = \frac{<P\hat{s}>}{P_n} = \frac{W\hat{s}/N\tau}{\sigma^2} = \frac{\parallel \hat{A}.exp(\hat{R},\hat{\omega},\hat{\alpha}) \parallel^2}{N\sigma^2}, \tag{2.31}$$

where N is the number of signal samples.

Chapter 3

Detection by means of Atmospheric Radar

3.1 Atmospheric radar for space debris detection

One of the application of radar is forecasting the conditions of the atmosphere. This is done by atmospheric radar. Atmospheric radars are used to monitor the situation in the atmosphere. Meteorological events such as wind and storm can be tracked and imaged by means of atmospheric radar [16].

Echoes from atmosphere are clutters, unwonted signals, in target detection such as for aircraft detection. Likewise echoes from space debris are clutter for atmospheric signal. This mens that detection of space debris is difficult using atmospheric radar. Since signal processors are designed in such a way that to remove clutters, which we are we are going to use detecting space debris. Therefore, the received copy after mixing the frequency of the radio wave must be stored not a separate storing device for processing the data [12 and 19].

Figure 3.1 shows atmospheric radar transmitting signal to the atmosphere. Here inthe diagram it is clearly seen that the signal reflected from satellites and space debris too. This makes possible using atmospheric radar to detect space debris.

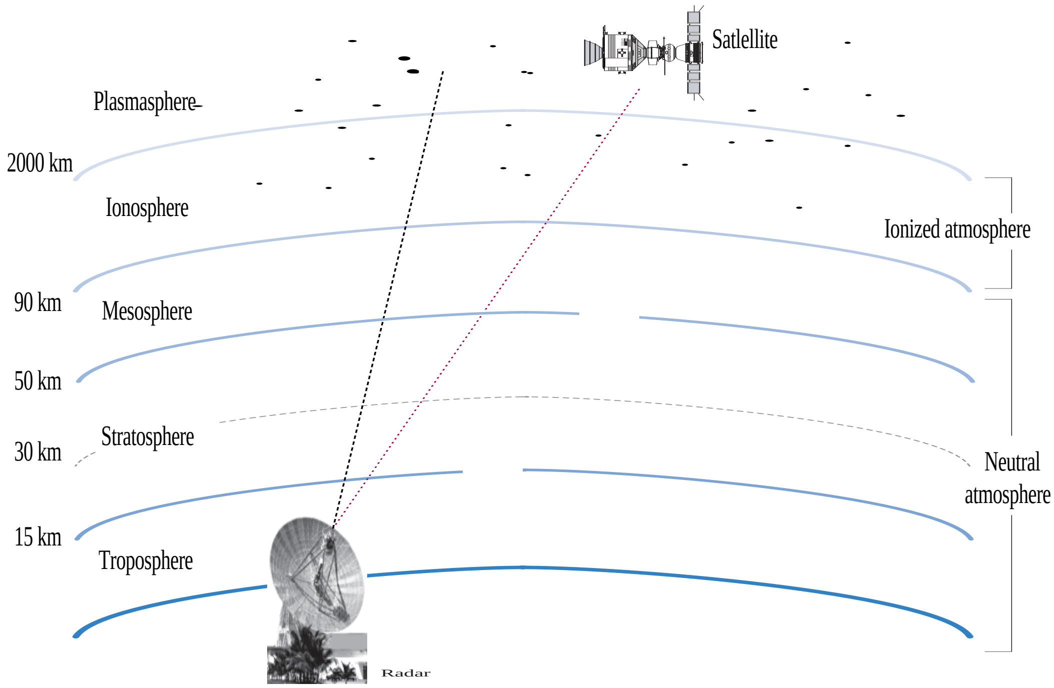

Figure 3.1: Atmospheric radar, radar beam and space debris near operational satellite.

3.2 Matched filter

There are variety of filtering techniques in signal processing. Matched filter is one of them which is characterized by its high signal-to-noise ratio (SNR). The matched filter is a from of correlation and it requires that a particular relationship exist between the spectrum of the transmitted signal and the frequency response of the receiver system [5, 6, and 7]. For a received signal $s(t)$, it can be shown that the frequency-response function of a linear, time invariant filter which maximizes the output SNR is given by

$$H(f) = S^*(f), \tag{3.1}$$

where $S(f)$ is the Fourier transform of $s(t)$, and $*$ indicate the complex conjugate. The filter whose frequency-response given by Eq.(3.1) is called matched filter, assuming the noise accompanying the received signal is random. For unknown received signal which is accompanied by white noise, the impulse response of the matched filter is assumed to be

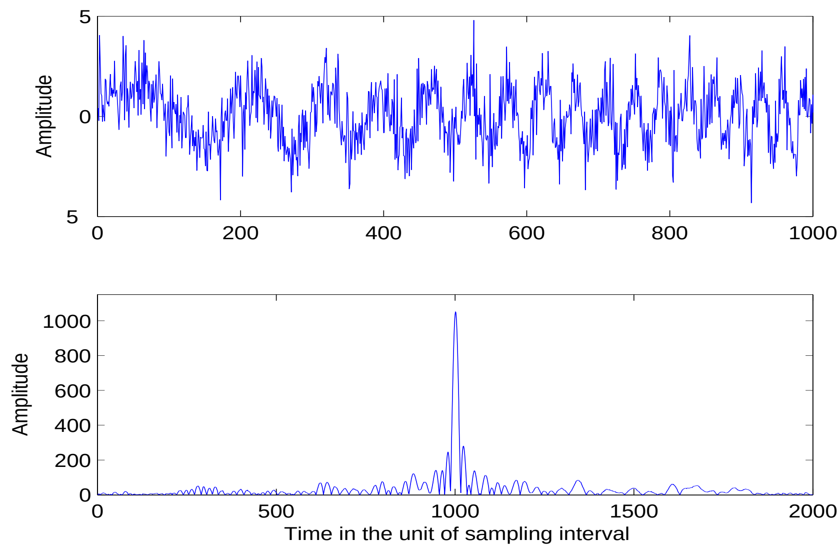

Figure 3.2: Matched filter. Top panel: the received signal. Bottom panel: the signal after matched filter.

the replica of the transmitted one [5, 17, and 18] and given by

$$h(t) = s^*(-t). \tag{3.2}$$

Figure 3.2 is generated using a simple periodic waveform with unknown additive noise and the principle of matched filter in applied.

3.3 Pulse compression

The peak transmitted power (P_t) of a radar can efficiently increase by increasing the pulse width of the transmitted signal. Increasing the pulse width of the transmission results a poor range resolution ($\Delta R = c\tau/2$), where τ is the pulse width. This means that a radar detects some close in inter-distance targets as a single object. The range resolution can effectively improve by decreasing the pulse width, which result low peak transmitted power. As a result the radar effective operational range reduce. Moveover the average transmitted power ($P_t\tau/T$), where T is the pulse repetition time, which is directly propor-

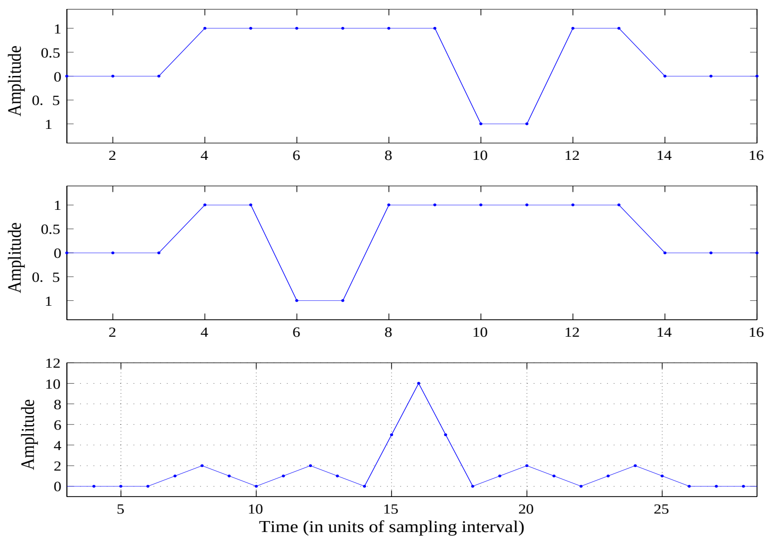

Figure 3.3: Pulse compression Barker code of 5-bit. Top panel shows the transmission code. Middle panel shows the replica of the code. Bottom panel shows the out put after pulse compression.

tional to peak transmitted power (P_t) is liked to SNR, the determining factor. For these problems radar designers employ pulse compression, also called pulse coding technique. Pulse compression provides for the transmission of a low peak-power, long-duration coded pulse and attain a good range resolution and improve detection performance of a short duration high peak-power pulse system. This is accomplished by coding the bandwidth of the transmitted pulse. Coding require decoding for filtering purpose. The analysis of measurements involves decoding made usually by means of matched filter [5, 6, and 7]. The demonstration of pulse compression using 5-bit Barker code shown in figure.3.3

3.4 Discussion of simulation result

The received signal in radar measurement contain many information about the target. In the case of space debris, we have shown in section (2.4) that one can infer the location (R), the velocity (v), and the acceleration (a) from the measured signal. Here we shall restrict our selves to the numerical investigation of space debris detection by means of atmospheric radar.

The signal one use to detect space debris may be dominated by the noise. This means that the received signal may be embedded in the noise. As a result detection of a debris particle would be very difficult. This be come horrible when the debris to be detected is very small in size. Since the received signal is directly related to the target radar cross section. And application like space debris detection demand high SNR. As we have discussed in section (3.2), a high SNR can be achieved employing a matched filter at the receiver output. The replica of the envelop of the transmitted signal is the impulse response of the matched filter.

3.4.1 Detecting space debris

Let us now consider the modulation envelop of the radar be a 13-bit Barker code given by

$$B_{13}(t) = env(t). \tag{3.3}$$

Figure 3.4 the first panel shows how the waveform described by Eq.(3.3) looks like. As one can see from Eq.(2.2) in section (2.4), the modulation envelop is carried by a carrier signal, which has very high frequency. However, this carrier is not needed in our numerical simulation. Because in practical measurement, the role of the carrier is to carry the waveform to the target and back. And at the receiver the carrier, by means of frequency mixing and typical low pass filter, is removed.

The next task is to model the impulse response $h(t)$, of our target. For simplicity, let us consider a waveform for the impulse response of the target as the random noise with single peak in the middle, as shown in figure 3.5. This true if the debris is large enough to dominate the scattering form the atmosphere. A similar result can be fund for small-sized object, with a modification the amplitude of the peak almost equal to that of the atmosphere.

The simulation of the measured radar signal is the convolution of the envelop of the

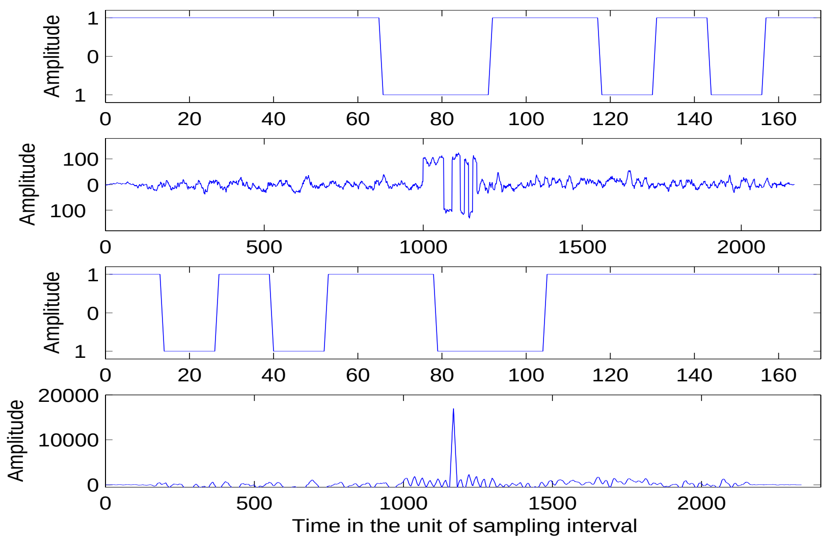

Figure 3.4: Demonstration detection of an object by atmospheric radar

transmission and the impulse response of the target, which is given by

$$M(t) = B_{13} * h(t). \tag{3.4}$$

This is shown in figure 3.4, third panel. The simulation result shown in figure 3.6 for small-sized gives no information. Unlike the larger objects the scattered signals from small-sized space debris appeared to be similar with the atmospheric signal. The scattering from the atmosphere can be assumed to be random, dominate the signals scattered from the small-sized space debris. As a result the measured signal seems to be random and detection of space debris is very difficult.

Here in this thesis we are interested to detect even small-sized space debris. Unlike the larger objects the scattered signals from small-sized space debris appeared to be similar with the atmospheric signal which can be assumed to be random, dominate the signal scatter from small-sized space debris. As a result the measured signal seems to be random and detection of small-sized space debris is very difficult. Applying the same simulation technique it turns out to be the debris is not detected, as shown in figure 3.6

As we can see from figure 3.6, in the case of small-sized space debris, the filtered output

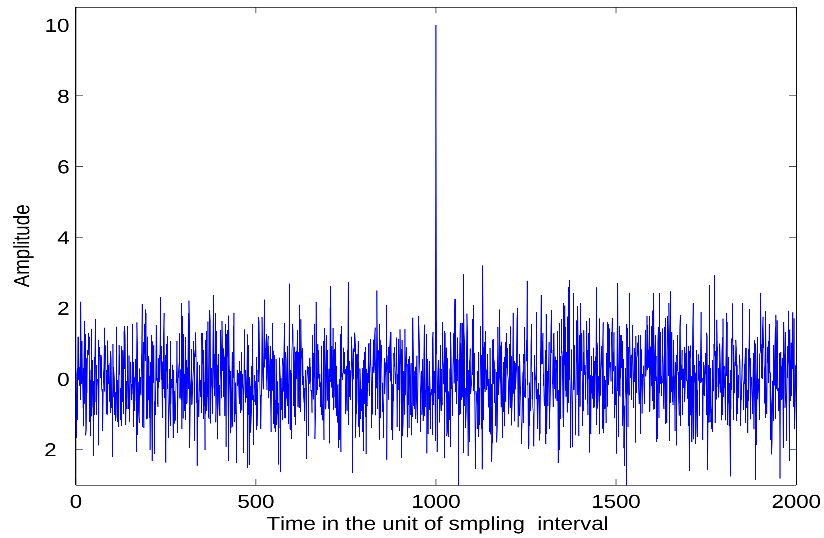

Figure 3.5: The impulse response of space debris in the atmosphere.

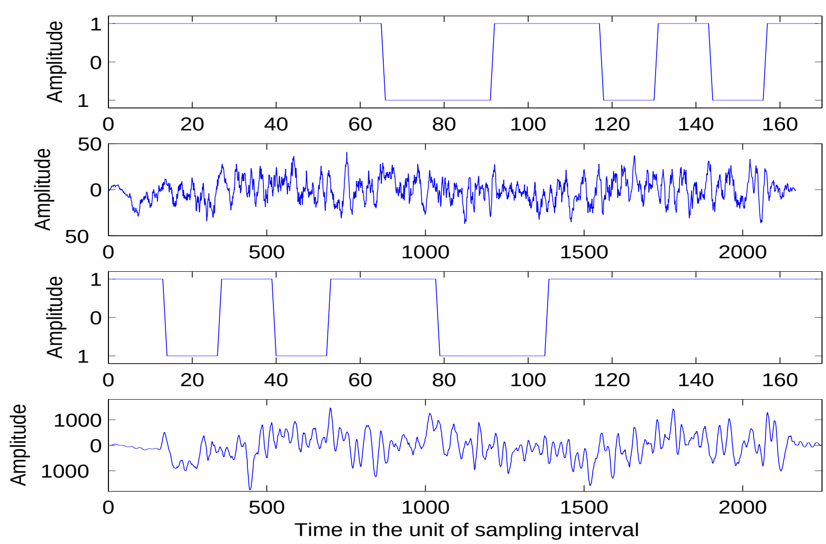

Figure 3.6: Unresolved debris detection by atmospheric radar. Top panel shows the code of the transmission. Second panel shows the measured signal. Third panel shows the replica of the code. Bottom panel shows the out put of the matched filter.

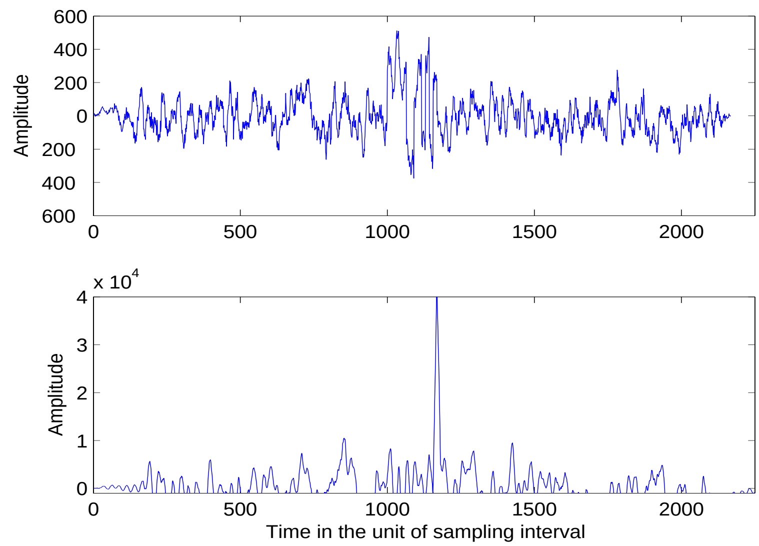

Figure 3.7: Small-sized debris detection by atmospheric radar. Top panel shows the sum of the measured signal. Bottom panel shows the output of the matched filter and integration.

which is expected to result a high SNR is immersed in the noise and therefore the debris is not yet detected. The scattered signals from the atmosphere can be assumed as a white noise. In such cases it is common knowledge to sum (integrate) up some successive pulses in the time of signal processing to detect the target clearly. Since the signal from the atmosphere is random, sum decrease the amplitude and goes to zero. And the signal from debris particle is not random so that the sum increase the amplitude. This description is applied in simulation and the result shown in figure 3.7

Further demonstration of space debris detection can be shown in the figure 3.8 and figure 3.9. The simulation here considers the motion of space debris. Since space debris are not stationary, it is worth to show how the detection evolves. We divided (discretized) the volume where the space debris is situated in ranges, layers of gates. As the time goes the debris particle jump from one gate to the next. This gives us how the range of the debris particle from the radar increase evolves. The change in range may be away from the radar, increase in range or to the radar, decrease in range.

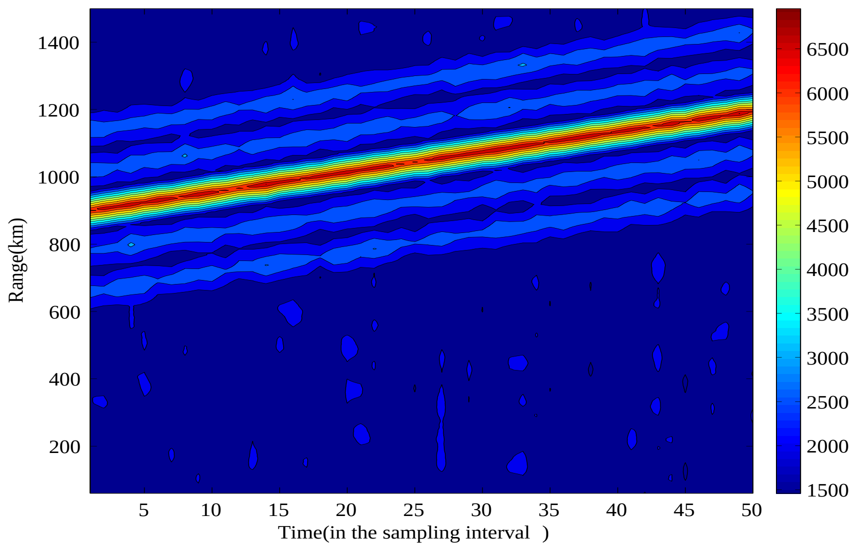

Figure 3.8: Evolution of space debris with range and time. Debris moving away from the radar.

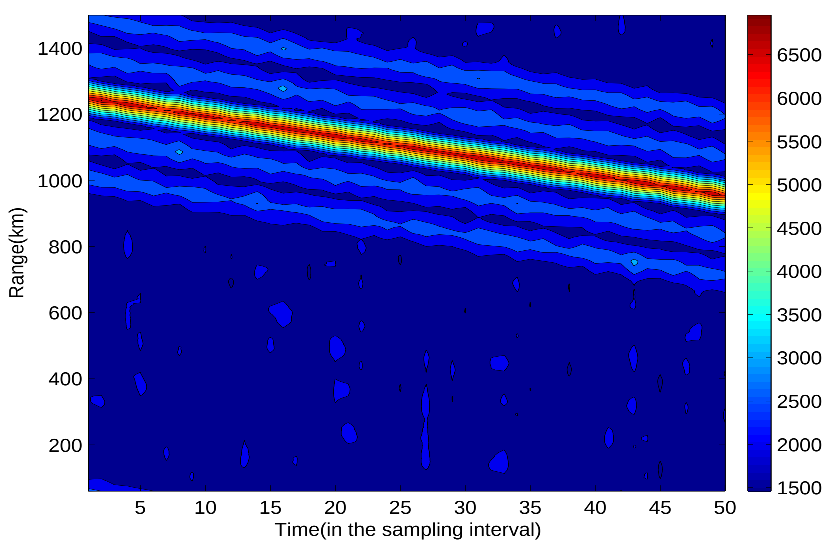

Figure 3.9: Evolution of space debris with range and time. Debris moving to the radar.

Chapter 4

Conclusions

Man-made orbital fragmentation may create great problem on operational satellite. Using the echo signal form the atmosphere we have show in this thesis how one can detect space debris. Since the back scattered signal from the atmosphere contain scattered signals from the space debris too, using atmospheric radar is possible in detecting a debris particle. We described the scattered signal from the space debris considered as clutter for atmospheric radar signal processor. Before the time of signal processing one has to store first the copy of the returned signal at the receiver separately. This make it possible to process the data from the atmospheric radar and detect the target, space debris.

Chapter 5

Future Directions

Space debris can be detected by means of atmospheric radar. This be made possible by storing the copy of the received signal from the atmospheric radar receiver separately. The work in this thesis concentrated on numerical simulation. A further project can be done employing the methods in this thesis on real data and additional investigation can be carried out to find out the parameters range, velocity, and acceleration of space debris using atmospheric radar.

Pulse integration of the measured signal from the atmospheric radar is used in this thesis to filter out the noise accompanying the signal. This can be tedious for the signal processor in terms of time consumption. One can carry out investigation to give out a system which can over come such a problem. This will give an alternative for measuring, detecting and monitoring space debris.

Bibliography

[1] Page, R. M.: The Origin of RADAR, Anchor Books, New York, 1962.

[2] Doviak, R. J., and Zrnic, D. S.: Doppler Radar and Weather Observations, Acadamic Press, 1993.

[3] U. S. War Department: Radar System Fundamental, 1944.

[4] Skolnik, M. I.: Intronuaction to Radar System, edited by S. Thyson, Academic press, New York, 1978.

[5] Ewell, W.: Radrr Transmitters, McGRAW-HILL Book Company, 1981.

[6] Mhafaz, R. B.: Radar Systems Analysis and Disning *Using* MATLAB, ACRC press campany, Boca Raton, 2000.

[7] Ridenour, L. N.: Radar System Engineering, McGRAN-HILL Books, 1947.

[8] Berkowitz, R. S.: Modern Radar Analysis, Evaluation, and System Design, *John Wiley and Sons, Inc.,* New York, 1965.

[9] Nygrén, T.: Introduction to Incoherent Scatter Measurements, INVERS publication, 1996.

[10] Mehrholz, D., Leashacka, L., Flury, W., Jehn, R., Klinkrad, H., and Landgraf, M.: Detecting, Tracking, and Imaging Space Debris, 2000.

[11] Technical Report on Space Debris, United Nations publication, New York, 1999.

[12] Maekkanen J., Lethinen, M., Huuskoner, A.: Measuerments of Small-Size Debris with Backscatter of Radio Waves, ESA contrate project, 2004.

[13] Bruyninekx, H.: Bayesian Probability, Belgium, 2000.

[14] Richard, C., Asten, Barches, B., and Thurber, C.: Parameter Estimation and Inverse Problem, 2004.

[15] Woodward, P. M.: Probability and Information Theory with Applications to Radar, Latimer Trend press, 1964.

[16] Woodman, R. F.: A General Statistical Instrument Theory of Atmospherical and Ionospheric Radars, *J. Geophys. Res.,* 96, 7911, 1991.

[17] Peterson, W. W., Birdsall, T. G., and Fox, W. C.: The Theory of Signal Detectability, *IRE Trans. Inform. Theory, PIGT-4,* 171, 1954.

[18] Kelly, E. J., Reed, I. S., and Root, W. L.: The Detection of Radar Echo in Noise II, *J. Soc. Ind. Appl. Math.,* 8(3), 481, 1960.

[19] Mudukutore, A. S., Chandrasekar, V., and Keeler, R. J.: Pulse Compression for Weather Radar. IEEE Transactions on Geosience and Remote Sensing, 36, 125, 1998.